

## Beta decay studies of the N=Z and waiting point nucleus $^{72}\text{Kr}$

J.A. Briz<sup>1,a</sup>, M.J.G. Borge<sup>1</sup>, E. Nácher<sup>1,2</sup>, A. Algora<sup>2</sup>, B. Rubio<sup>2</sup>, and the IS370 collaboration<sup>3</sup>

<sup>1</sup>*Instituto de Estructura de la Materia, CSIC, E-28006 Madrid, Spain*

<sup>2</sup>*Instituto de Física Corpuscular, CSIC-Univ. Valencia, E-46071 Valencia, Spain*

<sup>3</sup>*ISOLDE, PH Department, CERN, CH-1211 Geneve 23, Switzerland*

**Abstract.** The  $\beta^+/\text{EC}$  decay of  $^{72}\text{Kr}$  has been studied by means of the Total Absorption gamma Spectroscopy technique in order to determine the Gamow-Teller strength B(GT) distribution. The comparison with theoretical predictions suggests a dominantly oblate deformation for the  $^{72}\text{Kr}$  ground state. The de-excitation of low-energy excited states in  $^{72}\text{Br}$  is studied via conversion electron spectroscopy. The conversion coefficients and multipolarities of 14 low-energy transitions are determined and the spin and parity of the levels involved are deduced.

### 1 Introduction

Nuclei in the mass region  $A \approx 70-80$  are predicted to exhibit sudden shape changes from prolate to oblate and then back to prolate while moving along the N=Z line [1], see figure 1. An unusual oblate deformation is predicted for the ground states of  $^{70}\text{Br}$  and  $^{72}\text{Kr}$ . The shape coexistence phenomenon was first proposed in this mass region for  $^{72}\text{Se}$  [2] and evidences for the nucleus of interest,  $^{72}\text{Kr}$ , were found [3]. The existence of a  $0^+$  shape isomer state at 671(2) keV in  $^{72}\text{Kr}$  was interpreted as the prolate band head state causing a prolate mixing amplitude for the ground state of  $\lambda = 0.1$  [4].

Hartree-Fock (HF) calculations [5] predict that the GT distribution depends on the shape for nuclei in the mass region  $A \approx 70-80$ . These predictions have been supported by calculations performed by P. Sarriguren [6] where several nearby minima in potential energy at different quadrupole deformations are predicted. The proximity in energy of these minima with different deformations is usually a sign of shape coexistence. The predicted B(GT) distributions corresponding to these minima are different. This fact gives the opportunity to deduce information on the ground state deformations for nuclei in the mass region, such as  $^{74}\text{Kr}$  [7] and  $^{76}\text{Sr}$  [8].

For nuclear astrophysics,  $^{72}\text{Kr}$  is interesting due to its key role in the rapid proton capture process (rp-process) of nucleosynthesis in explosive environments. It is one of the so-called “waiting points” since the next nucleus in the proton capture path is  $^{73}\text{Rb}$ , which is unbound, making the process to slow down while the competition between 2 proton capture and  $\beta$  decay processes is at play. A careful study of the  $\beta$  decay properties of these “waiting point” nuclei in terrestrial conditions is crucial to perform reliable astrophysical network calculations, specially for weak interaction rates [9].

---

<sup>a</sup>e-mail: joseabriz@gmail.com

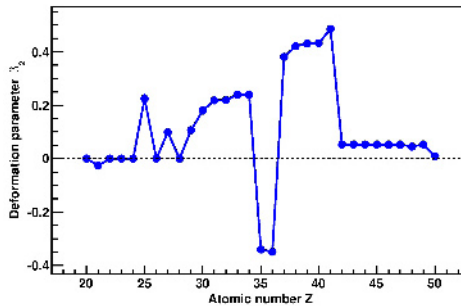


**Figure 1.** Theoretical predictions for the quadrupole deformation parameter  $\beta_2$  for the ground state of  $N=Z$  nuclei in the mass region  $A=40-100$  [1]. Strong shape changes are expected when moving from  $Z=34$  to  $Z=35$  (prolate to oblate) and from  $Z=36$  to  $Z=37$  (oblate to prolate). The only predicted cases with a strong oblate deformation are  $Z=35,36$ , i.e.  $^{70}\text{Br}$  and  $^{72}\text{Kr}$ .

## 2 Total Absorption gamma Spectroscopy technique

The purpose of this work is to determine the experimental distribution of GT strength in the full  $Q_\beta$  window. For this aim, the Total Absorption gamma Spectroscopy (TAS) technique has been used. The main advantage of this technique is that it overcomes the so-called Pandemonium effect present when performing High Resolution spectroscopy studies [10]. This technique makes use of a large crystal of scintillation material, in our case a cylindrical NaI(Tl) mono-crystal of 38 cm base diameter and 38 cm long, ideally covering the  $4\pi$  of solid angle around the radioactive source.

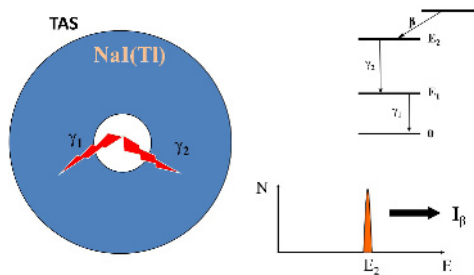


**Figure 2.** Total Absorption Spectrometer detector scheme. Individual  $\gamma$  radiations emitted by the source are added and the resulting spectra shows a peak located at the sum energy in the spectrum. Thus, the measurement of cascade intensities provide us with the beta feeding to the level from which the cascade was initiated.

The key idea is to be sensitive to the whole de-excitation gamma cascade following the beta decay process, see figure 2. Thus, instead of measuring individual gamma-rays one deduces the beta feeding intensities by measuring the gamma de-excitation intensity from the directly fed levels. The beta feeding would be obtained directly by integrating the peaks in the spectrum. However, the analysis gets tougher due to the fact that the real TAS efficiency is less than 100 %. This is mainly because a hole in the crystal is needed to place the sample and some ancillary detectors, like HPGc and a  $\beta$ -particles detectors to identify components in the samples.

### 3 Analysis

The analysis of the TAS spectrum consists of solving the expression linking the experimental data in each bin  $i$ ,  $d(i)$ , with the feeding distribution of the decay of interest in every bin  $j$ ,  $f(j)$ , which can be mathematically expressed as:

$$d(i) = \sum_j R(i, j) \otimes f(j) \quad (1)$$

where  $R(i, j)$  is the response matrix of the TAS detector to the decay of interest. It is important to note that both, the experimental spectrum and the decay scheme are fragmented in bins, labelled as  $i$  and  $j$  respectively, of a certain width (40 keV in our case). By inverting the  $R(i, j)$  matrix one should obtain the wanted feeding distribution  $f(j)$  and, consequently, the distribution of GT strength. The main difficulty comes from the fact that, in general, the  $R(i, j)$  matrix is not regular so the inversion has to be performed through mathematical algorithms. The Maximum Entropy (ME) and Expectation-Maximization (EM) algorithms were found to be the most suitable for the analysis in the comparison performed in [11]. The response matrix is obtained performing GEANT4 simulations of the experimental setup to calculate the behaviour of the TAS detector to the radiation involved in the decay of interest, namely  $\gamma$  radiation and positrons in the energy range from 0 up to the  $Q_\beta$ . This calculated response is validated using standard calibration sources.

Once the analysis is performed, a comparison of the experimental TAS spectrum  $d(i)$  with the re-constructed one, obtained from the convolution of the Response Matrix  $R(i, j)$  with the resulting feedings  $f(j)$ , is done in order to check the quality of the results. Figure 3 shows this comparison in the upper panel and the relative deviations  $[d_i - \sum_j R(i, j) \otimes f(j)]/d_i$  in the lower one. These results confirm the reliability of the feeding distribution found in the analysis.

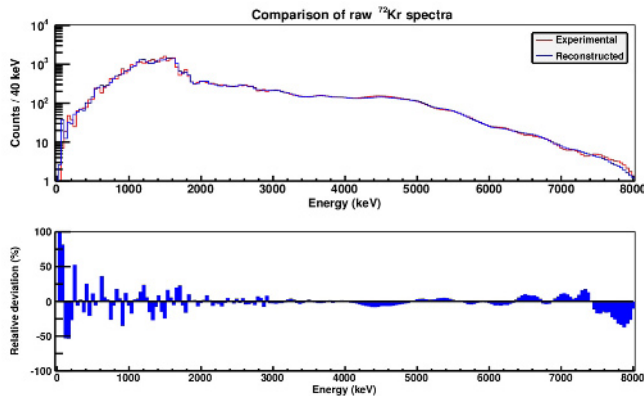


**Figure 3.** Comparison of experimental and re-constructed TAS spectra for the measurement of  $^{72}\text{Kr}$  decay. Deviations are reasonable in the full energy range confirming the reliability of the  $\beta$  feeding distribution obtained.

A good knowledge of the level scheme of the daughter nucleus is required for the analysis of the TAS spectrum. Information such as level excitation energies and spin-parities, de-excitation branching ratios and conversion coefficients of transitions is needed. Normally, this set of information is known up to a certain energy level. At higher excitation energies, one usually makes use of statistical models whose influence in the final result was studied in [12].

In the case of  $^{72}\text{Kr}$  decay scheme important information was missing: the spin-parity of most of the low excitation energy levels, including the ground state, were undefined and almost no conversion

coefficients were measured. Therefore, a study of the low-energy transitions in  $^{72}\text{Br}$  populated in the beta decay of  $^{72}\text{Kr}$  was done using a Miniorange spectrometer together with a Si(Li) detector for conversion electron detection and a HPGe detector for  $\gamma$ -rays.

## 4 Results

The study of conversion coefficients provides us with 14 conversion coefficients of low-energy transitions which help to deduce their multipolarities and the spin and parity of the levels involved. These results were included as input information in the analysis of TAS data.

From the resulting  $\beta^+$ -feeding distribution obtained in the  $\beta$ -gated analysis, the total ( $\beta^+$ +EC) feeding distribution is deduced and transformed into the GT decay strength in units of  $g_A^2/4\pi$ . Some preliminary values of the accumulated GT strength are given in table 1 in comparison with theoretical predictions for oblate and prolate deformations calculated using the SLy4 Skyrme force in [6]. These preliminary results suggest a dominantly oblate deformation for the  $^{72}\text{Kr}$  ground state. Additionally, this measurement validates the calculations in [6, 13] reinforcing the suggestion in [13] that continuum EC rates are comparable or even higher than  $\beta^+$  decay rates at rp-process conditions and they cannot be neglected as before [14].

**Table 1.** Preliminary results for the experimental accumulated B(GT) distribution of  $^{72}\text{Kr}$   $\beta^+$ /EC decay and theoretical predictions using SLy4 force [6] assuming oblate and prolate deformations for the  $^{72}\text{Kr}$  ground state.

$E_{exc}$ in $^{72}\text{Br}$ (keV)	Experimental $\sum B(GT)$ ( $g_A^2/4\pi$ )	Predicted $\sum B(GT)$ ( $g_A^2/4\pi$ ) [6]	
		Oblate	Prolate
0 - 100	0.010 $^{+0.008}_{-0.006}$	0.019	0.0073
0 - 500	0.18 $^{+0.03}_{-0.02}$	0.21	0.15
0 - 1100	0.34 $^{+0.03}_{-0.03}$	0.27	0.71
0 - 1500	0.48 $^{+0.02}_{-0.03}$	0.49	1
0 - 2100	0.80 $^{+0.04}_{-0.02}$	0.66	1.2
0 - 2700	1.07 $^{+0.07}_{-0.09}$	1.1	1.4

## References

- [1] P. Möller et al., Atomic Data and Nuclear Data Tables **59**, 185 (1995)
- [2] J.H. Hamilton et al., Phys. Rev. Lett. **32**, 239 (1974)
- [3] B.J. Varley et al., Phys. Lett. B **194**, 463 (1987)
- [4] E. Bouchez et al., Phys. Rev. Lett. **90**, 082502 (2003)
- [5] I. Hamamoto and X.Z. Zhang, Zeit. Phys. A **353**, 145 (1995)
- [6] P. Sarriguren et al., Phys. Rev. C **79**, 044315 (2009)
- [7] E. Poirier et al., Phys. Rev. C **69**, 034307 (2004)
- [8] E. Náchter et al., Phys. Rev. Lett. **92**, 232501 (2004)
- [9] K. Langanke and G. Martínez-Pinedo, Rev. Mod. Phys. **75**, 819 (2003)
- [10] J.C. Hardy et al., Phys. Lett. B **71**, 307 (1977)
- [11] J.L. Taín, D. Cano-Ott, Nucl. Inst. and Meth. A **571**, 728 (2007)
- [12] J.L. Taín, D. Cano-Ott, Nucl. Inst. and Meth. A **571**, 719 (2007)
- [13] P. Sarriguren, Phys. Rev. C **83**, 025801 (2011)
- [14] H. Schatz, Phys. Rep. **294**, 167 (1998)